

OPTICALLY-SWITCHED RESONANT TUNNELING DIODES FOR SPACE-BASED OPTICAL COMMUNICATION APPLICATIONS

71180

T.S. Moise, Y.-C. Kao, D. Jovanovic, and P. Sotirelis
Corporate Research and Development
Texas Instruments Inc., Dallas, TX 75265

ABSTRACT

We are developing a new type of digital photoreceiver that has the potential to perform high speed optical-to-electronic conversion with a factor of 10 reduction in component count and power dissipation. In this paper, we describe the room-temperature photo-induced switching of this InP-based device which consists of an InGaAs/AlAs resonant-tunneling diode integrated with an InGaAs absorber layer. When illuminated at an irradiance of greater than 5 Wcm^{-2} using $1.3 \mu\text{m}$ radiation, the resonant-tunneling diode switches from a high-conductance to a low-conductance electrical state and exhibits a voltage swing of up to 800 mV.

1. Introduction

Relative to conventional wire or cable technologies, optical fiber communication systems offer reduced weight, higher bandwidth and freedom from electromagnetic interference.¹ These attributes are particularly important for space-based applications in which reduced weight and power dissipation as well as electromagnetic interference immunity are critical. In recent years, satellite-based optical links have been demonstrated² and high-speed fiber optic networks for space-based data bus applications have been developed.³

The bandwidth, sensitivity, cost, and power consumption of a fiber optic communication system are controlled to a large extent by the characteristics of the optical receiver unit. Conventional receivers for these applications employ hundreds of transistors and consist of three primary subsystems: a photodetector, a low-noise amplifier, and a level-restoring comparator. For high-speed, long distance telecommunication systems, it is necessary to use a detector made from InGaAs which efficiently absorbs photons at the minimum dispersion and loss wavelengths of the optical fiber. A high speed, transimpedance amplifier, typically made from GaAs-based circuits, converts the optically induced photocurrent to a voltage signal which is then digitized. For high speed systems ($> 1 \text{ Gb/s}$), more than 1 W of electrical power is required to convert the incident optical signal to its electronic equivalent.

In this paper, we describe the room-temperature photoinduced switching of an InP-based device which consists of an InGaAs/AlAs resonant-tunneling diode integrated with an InGaAs absorber layer. When illuminated at an irradiance of greater than 5 Wcm^{-2} using $1.3 \mu\text{m}$ radiation, the resonant-tunneling diode switches from a high-conductance to a low-conductance electrical state and exhibits a voltage swing of up to 800 mV. The switching characteristics are reversible and, in the absence of light, the detector returns to its original high conductance operating state.⁴

2. Description of Device Operation

A schematic device cross-section and computed energy band diagram⁵ for the ORTD are shown in Figs. 1 and 2, respectively. The epitaxial layers employed in these experiments have been grown by molecular beam epitaxy using elemental group III and group V sources.⁶ As shown in Fig. 1, a thick $0.5 \mu\text{m}$ n^+ ($5 \times 10^{18} \text{ cm}^{-3}$) $\text{In}_{0.53}\text{Ga}_{0.47}\text{As}$ layer is epitaxially grown on the InP semi-insulating substrate. Following this heavily doped region, a lighter doped, 30 nm thick n-type ($1 \times 10^{18} \text{ cm}^{-3}$) $\text{In}_{0.53}\text{Ga}_{0.47}\text{As}$ layer is deposited followed by 100 nm of undoped $\text{In}_{0.53}\text{Ga}_{0.47}\text{As}$ which serves both to absorb the incident photons and to increase the peak-to-valley voltage swing of the diode.

An AlAs/ In_{0.53}Ga_{0.47}As/ AlAs (28 Å/ 50 Å/ 28 Å) RTD is then grown on the undoped In_{0.53}Ga_{0.47}As. Following the RTD, a thin (2 nm) In_{0.53}Ga_{0.47}As spacer layer, a 30 nm n-type (1 × 10¹⁸ cm⁻³) In_{0.53}Ga_{0.47}As layer, and 250 nm of n-type (5 × 10¹⁸ cm⁻³) In_{0.52}Al_{0.48}As are subsequently deposited. A thin (400 Å) n+ (5 × 10¹⁸ cm⁻³) InGaAs cap layer is then grown on top of the device. This emitter structure serves to minimize optical absorption within the top contact layers while maintaining a relatively low contact resistance of approximately 1 × 10⁻⁵ Ωcm², as derived by mesa-etched transmission line data. To minimize parasitic effects, we have employed airbridge contacts to the mesa-isolated ORTD devices.

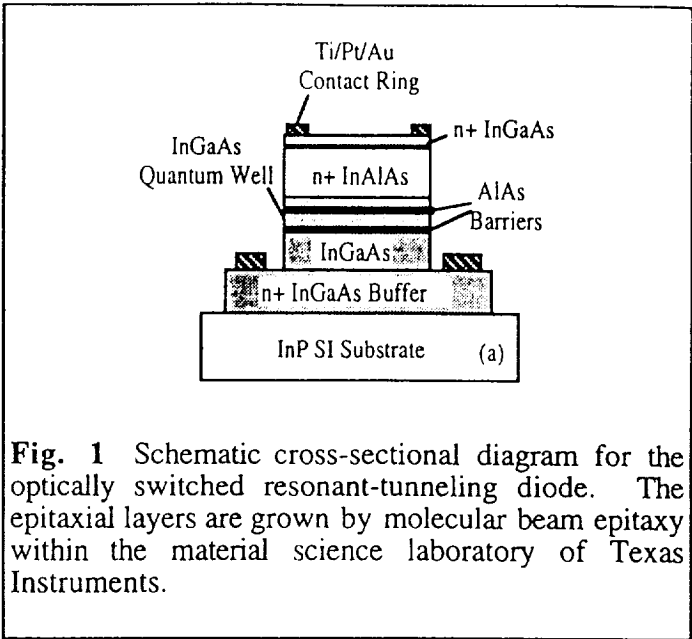


Fig. 1 Schematic cross-sectional diagram for the optically switched resonant-tunneling diode. The epitaxial layers are grown by molecular beam epitaxy within the material science laboratory of Texas Instruments.

The physical basis for ORTD operation can be explained with reference to the energy band diagram shown in Fig. 2 with 1.5 V applied bias. The external voltage is dropped primarily across the 100 nm undoped InGaAs layer because the width of this undoped layer is much larger than that of the double barrier structure (approximately 10 nm). For photon energies greater than 0.75 eV, electron hole pairs are created within this undoped layer. Under the influence of the external electric field, the photo-generated electrons are accelerated toward the n+ collector while the holes accumulate at the collector barrier of the ORTD. This process is similar to that described by England et. al.⁷ The accumulated charge partially neutralizes the electric field within the undoped layer which, in turn, leads to a local enhancement of the electric field within the double barrier structure. As a result, the current-voltage characteristics for the illuminated ORTD are shifted to lower voltage relative to the dark response.

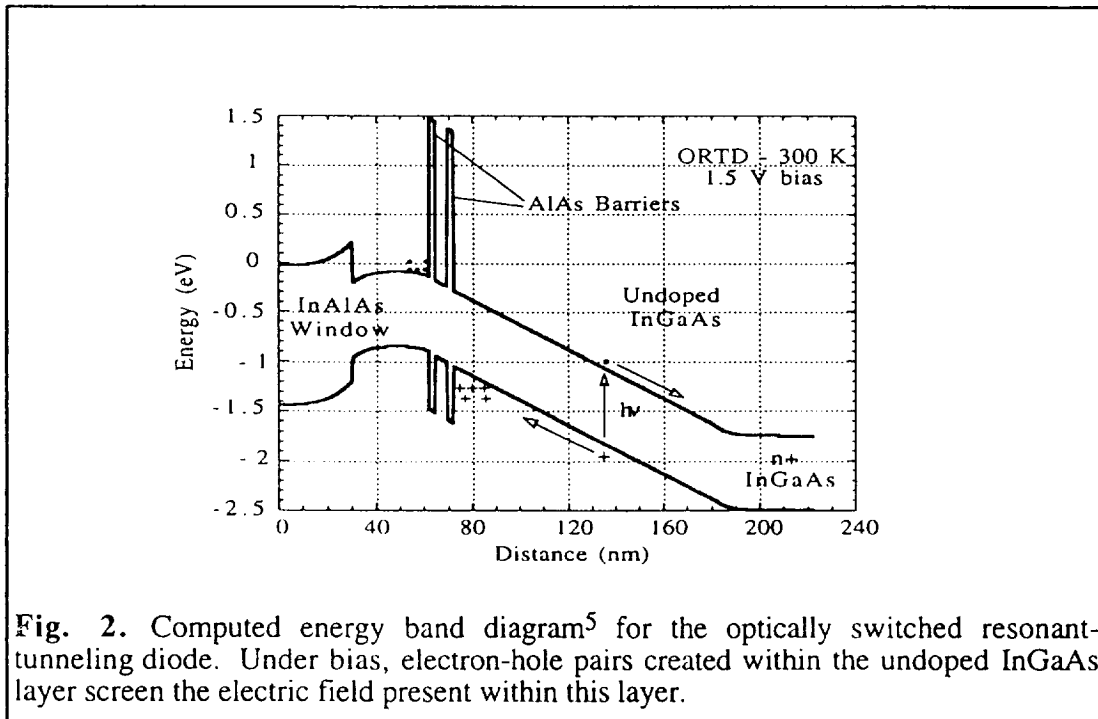


Fig. 2. Computed energy band diagram⁵ for the optically switched resonant-tunneling diode. Under bias, electron-hole pairs created within the undoped InGaAs layer screen the electric field present within this layer.

3. Experimental Results

Under dark conditions, the 60 μm diameter ORTD exhibits a peak voltage and current of 1.7 V and 24 mA, respectively, as depicted by the solid curve in Fig. 3. This bias polarity corresponds to electron injection from the surface towards the substrate. With light incident upon the ORTD, the magnitude of both the peak and the valley voltage are reduced as the result of electric field screening within the undoped intrinsic region. Thus, with an incident power of 1.0 mW at 1.3 μm , corresponding to an irradiance of 30 Wcm^{-2} , the peak voltage and the valley voltage are reduced by approximately 140 mV and 120 mV, respectively.

From this reduction in peak voltage, we can obtain an order-of-magnitude estimate for the steady state density of photogenerated holes in the following manner. First, we estimate the photo-induced reduction in electric field by dividing the observed voltage shift by the undoped spacer layer thickness. Second, we calculate the density of accumulated holes by using an infinite sheet charge approximation. Thus, from the measured 100 mV shift in peak voltage, we determine that the electric field is reduced by 1×10^4 V/cm within the 100 nm spacer layer leading to an estimated accumulated hole density of $6 \times 10^{10} \text{ cm}^{-2}$. To a first approximation, we anticipate that the accumulated hole density and the corresponding voltage shift will vary linearly

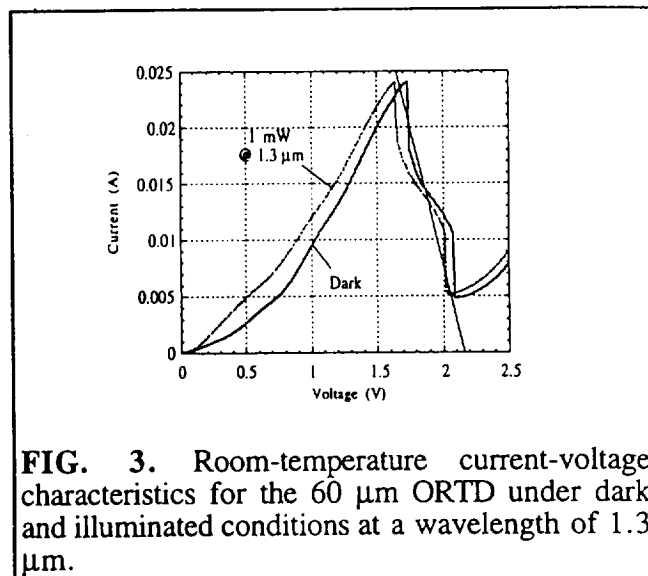


FIG. 3. Room-temperature current-voltage characteristics for the 60 μm ORTD under dark and illuminated conditions at a wavelength of 1.3 μm .

with irradiance. However, at high irradiance ($> 100 \text{ Wcm}^{-2}$), the experimental results suggest that hole tunneling through the double barrier structure, as evidenced by an increased valley current during illumination, leads to a saturation of the observed voltage shift. For negative polarity, we note that the peak voltage and current are nearly independent of irradiance as the result of electron accumulation at the InGaAs/AlAs interface.⁸

When biased with a resistor load, this photo-induced voltage shift is used to switch the device from a high-conductance to a low-conductance operating state, as illustrated by the load line drawn in Fig. 3. The bias values, $V_{\text{applied}} = 2.2 \text{ V}$ and $R = 20 \Omega$, are selected such that the load line intersects the dark current voltage characteristic near the peak voltage and intersects the illuminated characteristic near the valley voltage. By biasing the ORTD in this manner, we have created a bistable optical-to-electronic converter which operates at 1.7 V (23 mA) in the dark and 2.1 V (6 mA) when illuminated with an irradiance above the threshold value (determined by the load line and photo-induced voltage shift) of 20 Wcm^{-2} . For this measurement, the ORTD was illuminated at approximately 5 Wcm^{-2} using 1.3 μm radiation. We note that the plateau region observed in the current-voltage characteristics between 1.7 V and 2.0 V results from measurement circuit instability (i.e. oscillation) and does not constitute a stable operating point of the detector.

A timing diagram showing the measured output voltage of an ORTD together with the input laser drive signal is shown in Fig. 4. Under dark conditions, the ORTD is in a high-conductance state leading to a low output voltage (1.7 V).

With illumination, the resonant-tunneling structure switches into a low-conductance state leading to a high output voltage (2.1 V). Thus, this single device exhibits an output voltage characteristic similar to the more complex multi-transistor receiver circuits which require an order of magnitude more active components.

We have measured the large signal switching characteristics of the ORTD at higher frequency with the results shown in Fig. 5. For this measurement, the ORTD is biased through an RF bias tee which leads to a pulse width of approximately 7 ns. On this scale, the transition times are found to be less than 1 ns. Additional experiments are currently underway to understand the pulse width dependence upon RF bias conditions. The high speed measurements yield an output voltage swing of nearly 800 mV, which is double the voltage swing achieved at low frequency. This occurs because, at high frequency, the output is capacitively coupled and the voltage swing is the product of the optically induced current change

through the ORTD (16 mA - see Fig. 3) and the 50 Ω input impedance of the oscilloscope.

In an attempt to estimate the upper limit for the ORTD large-signal switching speed, we have measured the on-wafer small signal response using a 20 μm diameter ORTD biased at 1.0 V through a 30 W resistor. The results are shown in Fig. 6. For these impulse measurements, the ORTD was illuminated with a 250 fs pulse at 1.3 μm generated using optical parametric amplifier system. The 3 dB bandwidth was found to be approximately 4 GHz. Additional tests with higher bandwidth emitters are currently underway to further characterize the frequency response limits of the ORTD.

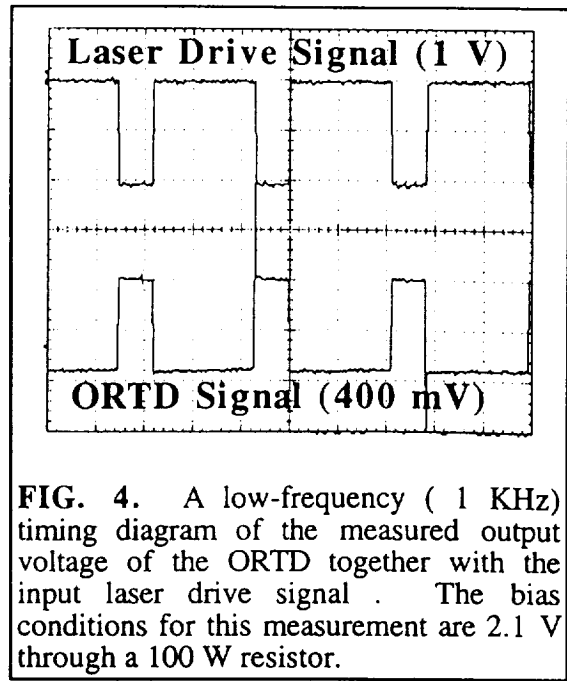


FIG. 4. A low-frequency (1 KHz) timing diagram of the measured output voltage of the ORTD together with the input laser drive signal . The bias conditions for this measurement are 2.1 V through a 100 W resistor.

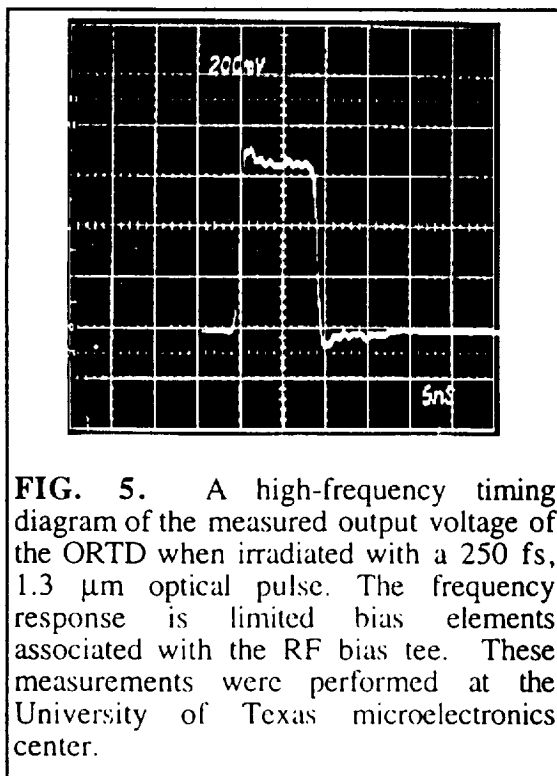


FIG. 5. A high-frequency timing diagram of the measured output voltage of the ORTD when irradiated with a 250 fs, 1.3 μm optical pulse. The frequency response is limited bias elements associated with the RF bias tee. These measurements were performed at the University of Texas microelectronics center.

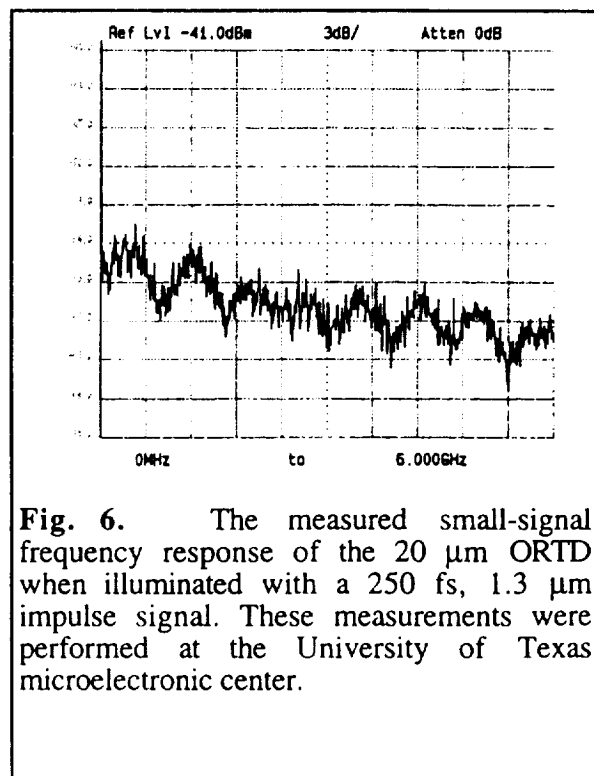


Fig. 6. The measured small-signal frequency response of the 20 μm ORTD when illuminated with a 250 fs, 1.3 μm impulse signal. These measurements were performed at the University of Texas microelectronic center.

4. Conclusions

In summary, we have developed an optically-switched, resonant-tunneling diode that exhibits up to a 800 mV output voltage swing when illuminated at an irradiance on the order of 5 Wcm^{-2} using $1.3 \mu\text{m}$ radiation. The switching characteristics are reversible and, in the absence of light, the detector returns to its original high conductance operating state. Small-signal optical measurements of the ORTD biased prior to resonance demonstrate a 3 dB bandwidth of approximately 4 GHz.

5. Acknowledgments

We gratefully acknowledge the assistance of Professor Joe Campbell of the University of Texas in performing the ultrafast impulse measurements. We also acknowledge many useful discussions with T.P.E. Broekaert, G.A. Frazier, and A.C. Seabaugh along with the outstanding technical assistance of E. Pijan and R. Thomason all of Texas Instruments.

REFERENCES

- 1) E.J. Friebele, M.E. Gingerich, and D.L. Griscom, SPIE **1791**, p. 177 (1992).
- 2) E.W. Taylor, J.H. Berry, A.D. Sanchez, R.J. Padden, S.P. Chapman, 1992 DOD Fiber Optics Conference Proceedings, p. 25 (1992).
- 3) J. Bristow and J. Lehman, SPIE **1953**, p. 159 (1993).
- 4) T. S. Moise, Y.C. Kao, L.D. Garrett, and J.C. Campbell, Appl. Phys. Lett., **66** (9) p. 1104 (1995).
- 5) BANDPROF heterojunction device simulator, W.R. Frensley, 1993.
- 6) Y.-C. Kao, A.C. Seabaugh, H.Y. Liu, T.S. Kim, M.A. Reed, P. Saunier, B. Bayraktaroglu, and W. M. Duncan, Proc. S.P.I.E. **1144** p. 30 (1989).
- 7) E.T. Koenig, C.I. Huang, and B. Jogai, J. Appl. Phys. **68** (11) p. 5905 (1990).
- 8) P. England, J.E. Golub, L.T. Florez, and J.P. Harbison, Appl. Phys. Lett., **58** (9) p. 887 (1991).

